Desalination and Water Treatment
www.deswater.com
doi: 10.1080/19443994.2015.1046148

57 (2016) 11972–11987
June

Taylor & Francis
Taylor & Francis Group

Modeling and optimization of a hybrid power system supplying RO water desalination plant considering CO_2 emissions

Ahmed Hassan, Magdi El-Saadawi, Mahmoud Kandil, Mohammed Saeed*

Faculty of Engineering, Electrical Engineering Department, Mansoura University, Mansoura, Egypt,
emails: arwaahmed1@gmail.com (A. Hassan), m_saadawi@mans.edu.eg (M. El-Saadawi), mahmoud.kandil@yahoo.com (M. Kandil), mohammedsaid@mans.edu.eg (M. Saeed)

Received 21 December 2014; Accepted 23 April 2015

ABSTRACT

Seawater desalination is an attractive choice especially for remote areas where freshwater is rare. Egypt is moving toward the desalination of water as an alternative solution to the decrease in freshwater. The main objective of this study was to design an optimal, economic, and efficient hybrid system that feeds the electric needs of a small-scale brackish reverse osmosis desalination unit and a tourism motel located in Hurghada, Egypt. The optimization problem of sizing different components of hybrid system is a complicated one; it needs a special tool capable of solving it rapidly and effectively. Three different hybrid system scenarios are discussed to select the most optimum combination of them. These scenarios are the following: wind/PV/battery, wind/PV/diesel, and wind/PV/battery/diesel. In this study, a modified particle swarm optimization technique is applied for optimum sizing of the proposed hybrid system scenarios. The optimization problem is solved to minimize the annual total investment cost considering CO_2 emissions cost.

Keywords: CO_2 emissions; Diesel generator; Hybrid systems; Photovoltaic; MPSO; Stand-alone; Wind turbines

1. Introduction

Freshwater supply in Egypt depends on Nile River, exploiting groundwater, reuse of treated wastewater, recycling of water irrigation, and desalination. Egypt experiences an annual water shortfall of 7 billion cubic meters, and domestic water demand in the country is expected to increase by 25% in 2025 [1]. Sea water desalination is a water treatment process that separates salts from saline water to produce potable water or water that is low in total dissolved solids. There are more than 15,000 industrial-scale desalination units had been installed in the world, and they account for a total capacity of more than 8.5 billion gallons/d [2]. In Egypt, most coastal areas are too far from the grid, so it is difficult to electrify desalination plants installed in those areas by the utility grid. Renewable energy sources represent an attractive option to solve this problem. In recent years, hybrid system is becoming popular for stand-alone power generation in isolated sites due to the advancement in renewable energy technologies and power electronic converters. In many regions, when solar and wind resources are combined for power generation, they complement each other by means of daily and seasonal variations. This combination reduces the dependence on one environment

*Corresponding author.

parameter, thus providing the consumer with reliable and cheap electricity, and is more effective than utilization of single renewable energy source [3].

In the past few years, several methods have been used to design the hybrid system for water desalination plants. In [4], the authors presented an experimental research facility for sea water osmosis desalination powered from a grid connected hybrid system at Libya coast. The authors in [5] used stochastic optimization software based on evolutionary algorithm for optimum design and operation strategy of a stand-alone hybrid system desalination scheme, capable of fulfilling the freshwater demand in remote coastal regions. A major disadvantage of stochastic optimization techniques is the large computational time. A simulation program based on visual basic programming language was used in order to achieve optimum design of a hybrid system—seawater desalination system in [6]. The disadvantages of visual basic include the fact that it normally requires lots of memory for initial installation and in order to function efficiently after installation. Authors in [7] presented a genetic algorithm applied for optimal design of a hybrid system used to supply RO desalination unit. The objective function is to minimize the total water cost. The feasible solutions are obtained through simulations carried along a complete year.

Recently, commercial software simulation tools are broadly used in performance assessment of hybrid system. These models are used to simulate the performance of hybrid systems that typically include one or more renewable sources of electricity combined with a traditional fossil fuel source. These models include the following: hybrid optimization model for electric renewable (HOMER), RETScreen, Hybrid2, TRNSYS, and many other software packages [8,9]. The most important one of these tools is the HOMER. It was applied in many articles to study different scenarios for the optimum sizing of hybrid system supplying RO desalination plants [10–16]. The main drawback of these software models is the "Black Box" code utilization.

The optimization problem of sizing different components of hybrid system is a complicated one; it needs a special tool capable of solving it rapidly and effectively. Particle swarm optimization (PSO) is one of the most promising artificial intelligence techniques for solving such optimization problems. It is easily implemented and has proven both very effective and quick when applied to a diverse set of optimization problems [17].

This study presents a methodology for optimal sizing of a stand-alone hybrid PV-wind power generation system coupled to a battery bank and/or a diesel generator to provide RO desalination unit and a tourism motel in Hurghada, Egypt, with their needs of electricity. Modified particle swarm optimization (MPSO) technique is applied for optimum sizing of three proposed hybrid system scenarios. An influence study of the CO_2 emission on the optimal system configuration is also presented.

2. RO desalination system power consumption

A reverse osmosis system consists of four major components/processes: (1) pretreatment, (2) pressurization, (3) membrane separation, and (4) post-treatment stabilization. Fig. 1 illustrates the basic components of a reverse osmosis system.

Power consumption by the system includes power for seawater pumping and high-pressure pumping. The power requirement of each pump is calculated using the following formula (1) [18]:

$$P_p = Q \cdot P_r/(\eta_p \cdot \eta_m) \quad (1)$$

where P_p—power consumed by each pump, kW; Q—feed water flow rates for each pump, m^3/s; P_r—feed water pressure of each pump, kPa; η_p—pump efficiency; and η_m—motor efficiency.

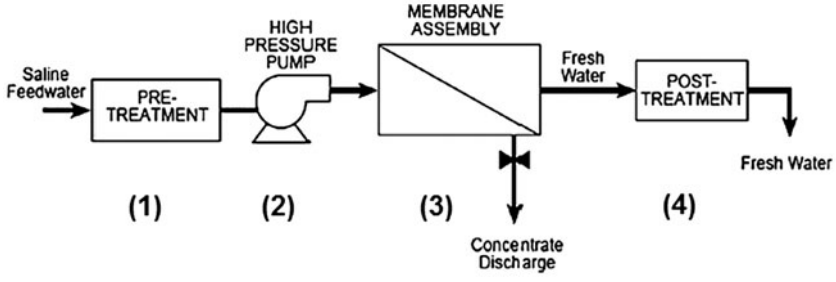

Fig. 1. Elements of a reverse osmosis desalination system.

3. Hybrid system components mathematical modeling

The proposed RO desalination system will be supplied by a hybrid PV-wind power generation system coupled to a battery bank and/or a diesel generator. The system consists of a PV module, a wind turbine, a PV controller, an inverter, a battery bank and/or a diesel generator. A schematic diagram of the proposed system is shown in Fig. 2. Mathematical modeling of the components is the first step for optimization process. In the following subsections, a brief description of hybrid system components modeling is explained.

3.1. Mathematical model of wind turbines

Power speed curve is the simple model to simulate the output power of a wind turbine [19]. It is important to adjust the measured wind speed to the hub height (h). This can be done by using the wind speed data at a reference height (h_r) from the database as explained by [20]:

$$v(t) = v_r(t) \cdot \left(\frac{h}{h_r}\right)^{\gamma} \tag{2}$$

where v is the wind speed at the desired height h, v_r is the wind speed at a reference height h_r, and γ is the wind shear exponent coefficient which varies with pressure, temperature, and time of day, ranging from 1/7 to 1/4 [20]. In this study, this coefficient is taken as one-seventh (1/7). Weibull probability distribution function is the most appropriate, accepted and recommended distribution function for wind speed data analysis. The probability density function indicates the probability of the wind at a given velocity. The Weibull probability density function is given as

$$f(x) = \frac{\beta}{\eta} \cdot \left(\frac{x}{\eta}\right)^{\beta-1} \cdot e^{-\left(\frac{x}{\eta}\right)^{\beta}} \tag{3}$$

where β is the shape factor; x is the wind velocity, and $x \geq 0$, $\beta > 1$, $\eta > 0$.

The scale factor η shows how the distribution lies and how it stretched out. The output power of wind can be calculated by using Weibull probability density function for a specific site. The output energy from the wind turbine, at any wind velocity, can be estimated by using wind turbine power curve which is usually given by manufacturer. For a wind speed profile, the available energy can be calculated as [21]:

$$E_{WT} = T_{hr} \cdot \sum_{v_{min}}^{v_{max}} P_c f(v, \beta, \eta) \tag{4}$$

where E_{WT} is the energy generated by the wind turbine at a specific site (in kWh), T_{hr} is the total hours used in simulation, P_c is the output power of wind turbine (in kW), v_{min} and v_{max} are the minimum and maximum wind speeds, and $f(v, \beta, \eta)$ is the Weibull probability density function for wind speed v at a given shape factor β and scale factor η.

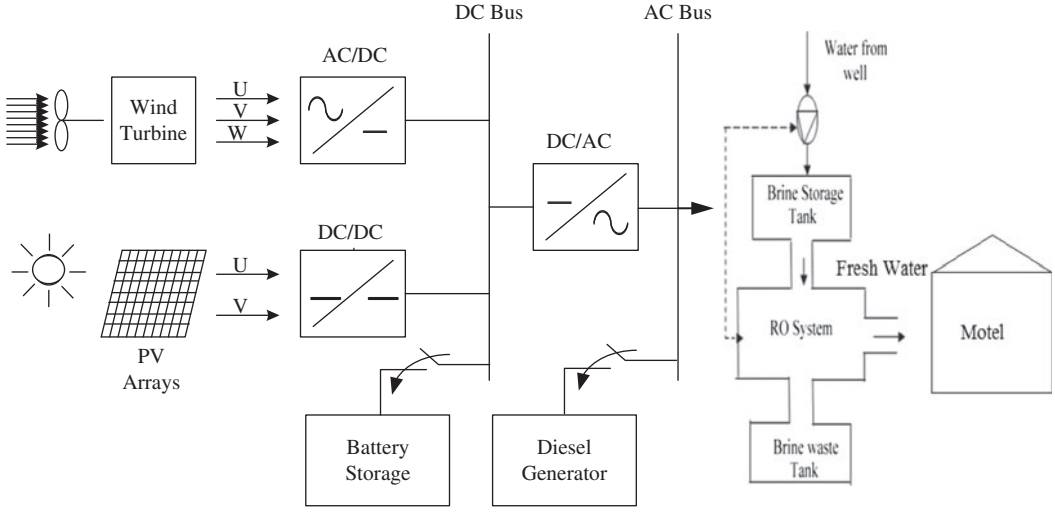

Fig. 2. Block diagram of the proposed hybrid system.

3.2. Mathematical model of PV modules

The PV array performance is simulated by deriving a PV model that represents the maximum output power at any temperature. The used model has to predict output power of PV panel at different temperatures and various radiation levels. The proposed mathematical model of a PV panel is deduced using the following equations [21]:

$$P_{PV} = V \cdot I(V) \tag{5}$$

where

$$I(V) = \frac{I_x}{1 - e^{\left(\frac{1}{b}\right)}} \cdot \left[1 - e^{A}\right] \tag{6}$$

$$A = \left(\frac{V}{b \cdot V_x} - \frac{1}{b}\right) \tag{7}$$

$$V_x = n_s \cdot \frac{E_i}{E_{iN}} \cdot \mathrm{TCV} \cdot (T - T_N) + s \cdot V_{max} - B \tag{8}$$

$$B = n_s.(V_{max} - V_{min}) \cdot e^{C} \tag{9}$$

$$C = \left(\frac{E_i}{E_{iN}} \cdot \ln\left[\frac{V_{max} - V_{oc}}{V_{max} - V_{min}}\right]\right) \tag{10}$$

$$I_x = n_p \cdot \frac{E_i}{E_{iN}}.[I_{sc} + \mathrm{TCI} \cdot (T - T_N)] \tag{11}$$

where P_{PV}—output power of the PV panel (W); $I(V)$—output current of the PV panel at a specific output voltage (A); V—output voltage of the PV panel (V); b—characteristic constant based on I–V curve, its value ranges from 0.01 to 0.18 [22]; SR_i—solar radiation impinging the cell (W/m^2); SR_{iN}—solar radiation at standard test condition (STC) (=1,000 W/m^2); T_N—temperature at STC (=25°C); I_{sc}—short circuit current at STC (A); V_{oc}—open circuit voltage at STC (V); V_{max}—open circuit voltage at 25°C and 1,200 W/m^2 (V); V_{min}—open circuit voltage at 25°C and 200 W/m^2 (V); T—temperature of PV panel (°C); T_{CI}—temperature coefficient of I_{sc} (A/°C); T_{CV}—temperature coefficient of V_{oc} (V/°C); I_x—short circuit current at any solar radiation and panel temperature (A); V_x—open circuit voltage at any solar radiation and panel temperature (V); n_s—number of PV panels in series; n_p—number of PV panels in parallel.

The following equation is used to calculate the annual energy of PV arrays at a specific site with a given solar radiation.

$$E_{PV} = P(SR_x) \cdot (SW) \cdot (365) \tag{12}$$

where E_{PV} is the annual production of PV energy, SW is the total hours the sun hits the PV module at an average hourly solar radiation, and $P(SR_x)$ is the PV module output power at an average hourly solar radiation SR_x.

3.3. Mathematical model of a battery bank

In the proposed hybrid system the lead acid batteries are used to store surplus energy, to regulate system voltage and to supply power to load in case of low wind speed and/or low solar conditions. The required battery bank capacity (B_R) for a hybrid system can be calculated using the following equation [23].

$$B_R = \frac{L_{Ah/d} \cdot N_C}{M_{DD} \cdot D_F} \tag{13}$$

where $L_{Ah/d}$—total Amp-hour consumed by the load in a day; N_C—number of autonomous days; M_{DD}—maximum depth of discharge; D_F—discharging factor.

The number of batteries to be connected in parallel (B_P) to give the Amp-hour required by the system is calculated as:

$$B_P = \frac{B_R}{B_C} \tag{14}$$

where B_R is the required battery bank capacity in (Ah) and B_C is the capacity of the selected battery in (Ah).

On other hand, the number of series batteries (B_S) required to achieve the system voltage is calculated by dividing the system DC voltage (V_N) by the battery voltage V_B [23]:

$$B_S = \frac{V_N}{V_B} \tag{15}$$

The total number of batteries (N_B) is obtained by multiplying the total number of batteries in series by the total number of batteries in parallel:

$$N_B = B_S \cdot B_P \tag{16}$$

Finally, the total cost of the battery bank C_{Bank} is computed as:

$$C_{Bank} = N_B \cdot C_B \tag{17}$$

where C_B is the retail cost of a battery.

3.4. Mathematical model of PV controller

The PV controller works as a voltage regulator. In this study, the maximum power point tracking MPPT controller is used as a PV controller. This controller tracks the maximum power point of the array throughout the day to deliver the maximum available solar energy to the system [23].

The selection of controllers must validate the following constraints:

$$V_{con\_max} \geq V_{PVmax} \tag{18}$$

$$V_{PVmax} = V_{oc} \times s \tag{19}$$

where V_{con_max} is the maximum controller voltage rating and V_{PVmax} is the maximum PV voltage.

The following equations are used to calculate the number of controllers (N_{con}) needed for a PV array system [23].

$$P_{PV\_S_{max}} = P_{PV\_S} \times N_{PV} \tag{20}$$

$$P_{con\_max} = V_B \times I_{con} \tag{21}$$

$$N_{con} = \frac{P_{PV\_S_{max}}}{P_{con\_max}} \tag{22}$$

where P_{PV_S} represents the rated power of the PV at STCs. The N_{PV} is the total number of PV module. I_{con} is the maximum current the controller can handle from the PV system to the battery bank.

3.5. Mathematical model of inverter

The power inverter is a key component in most alternative energy systems. Inverters are commonly used as the interface to connect the renewable energy sources and the load. The normal output of an inverter is a sine wave with the required frequency. Inverters are available in three different categories: grid-tied batteryless inverters and grid-tied with battery backup and stand-alone inverters. The stand-alone inverters are designed for independent utility-free power system and are appropriated for remote hybrid system installation. Inverters convert DC power from batteries or solar modules into usable AC power to supply the load. These inverters have battery charge capability to keep the batteries fully charged and ready to use. The number of inverters needed for the hybrid energy system, is calculated as:

$$N_{IN} = \frac{P_{G\_max}}{P_{IN\_max}} \tag{23}$$

where P_{G_max} represents the maximum generated power by the hybrid system and P_{IN_max} is the maximum power that can be supplied by the inverter.

3.6. Mathematical model of diesel generator

In this study, a diesel generator is assumed to share the PV/wind generation system to feed the load. For better performance and higher efficiency, the diesel generators will always operate between 80 and 100% of their nominal ratings. Energy generated by a diesel generator is calculated as [24]:

$$E_{DG}(t) = P_{DG}(t) \times \eta_{DG} \times t \tag{24}$$

where $E_{DG}(t)$ is the hourly energy, P_{DG} is the rated power, η_{DG} is the efficiency of diesel generator, and t represents its operation time.

The fuel consumption of a diesel generator depends on the generator size and the load at which the generator is operating. The fuel cost of the diesel generator can be modeled as a quadratic function [24]

$$C_{f\_DG} = C_f(\propto P_N + \beta P_o) \tag{25}$$

where C_f is the fuel price in ($/L) including fuel transportation, α and β are the coefficients of fuel consumption curve, and P_N and P_o are nominal capacity and power output of the diesel generator, respectively. In this study, α and β are taken as 0.081451 and 0.2461 L/kWh, respectively, [23] and C_f equals $0.4/L [25].

The total amount of CO_2 emission can be calculated as [26]:

$$Q_{CO_2} = FC \times EF \tag{26}$$

where Q_{CO_2} is the total amount of CO_2 emission in kg, FC is the fuel consumption in kWh, and EF is the emission factor for the fuel used in kg/kWh. For the diesel fuel used in this study the default effective CO_2 emission factor is 0.705 kg/kWh [26].

Egypt does not impose a tax on carbon dioxide emissions in any sector, whether industrial or energy production. But the Ministry of Environment recommended that according to the Environmental Law No. 4 to 1994 there is a need to impose such a tax for the annual emissions of that harmful gas. The Ministry of Environment calculated these values according to European standards in [27].

4. Optimal design model of stand-alone hybrid system

The optimal combination of a hybrid solar–wind–diesel–battery system makes the best compromise between the system pollutant emission and the cost of energy to minimize the system investment cost through the system lifetime.

4.1. Objective function

The objective function in this study is to minimize the system total investment cost (TIC) through the system lifetime (T_{life}). The unknown variables are the number of PV modules, wind turbines, battery banks, inverter units, controllers units, and diesel generators. These variables represent the number of equipment needed to supply the load at minimum investment cost. The problem is solved for three scenarios: PV/wind with battery storage, PV/wind with diesel generator, and PV/wind/diesel with battery storage. The objective function can be formulated mathematically as follows:

4.1.1. Minimize

$$\begin{aligned}\mathrm{TIC} = &\sum_{i=1}^{n_{\mathrm{PV}}}(C_{\mathrm{PV}i}N_{\mathrm{PV}i}) + \sum_{j=1}^{n_{\mathrm{wt}}}\left(C_{\mathrm{WT}j}N_{\mathrm{WT}j}\right) + \sum_{k=1}^{n_{\mathrm{bat}}}(C_{\mathrm{Bat}k}N_{\mathrm{Bat}k}) \\ &+ \sum_{l=1}^{n_{\mathrm{inv}}}(C_{\mathrm{IN}l}N_{\mathrm{IN}l}) + \sum_{m=1}^{n_{\mathrm{con}}}(C_{\mathrm{CON}m}N_{\mathrm{CON}m}) \\ &+ \sum_{z=1}^{n_{\mathrm{DG}}}(C_{\mathrm{DG}z}N_{\mathrm{DG}z})\end{aligned} \tag{27}$$

where C_{PV}, C_{WT}, C_{Bat}, C_{IN}, C_{CON}, and C_{DG} are TICs for each type of PV module, a wind turbine, battery bank, an inverter, a controller, and diesel generator, respectively.

N_{PV}, N_{WT}, N_{Bat}, N_{IN}, N_{CON}, and N_{DG} are number for each type of PV modules, wind turbines, battery banks, inverter units, controllers units, and diesel generators, respectively.

The TIC for each component except diesel generator includes capital cost (C_{cap}), installation cost (C_{ins}), and annual operation and maintenance cost ($C_{O\&M}$). The TIC of diesel generators includes capital cost (C_{cap}), installation cost (C_{ins}), annual operation and maintenance cost ($C_{O\&M}$), fuel cost (C_f), and CO_2 emissions cost (C_{em}).

$$C_{\mathrm{PV}} = C_{\mathrm{cap\_pv}} + C_{\mathrm{ins\_pv}} + T_{\mathrm{life}} \times C_{\mathrm{O\&M\_pv}} \tag{28}$$

$$C_{\mathrm{WT}} = C_{\mathrm{cap\_wt}} + C_{\mathrm{ins\_wt}} + T_{\mathrm{life}} \times C_{\mathrm{O\&M\_wt}} \tag{29}$$

$$C_{\mathrm{Bat}} = C_{\mathrm{cap\_Bat}} + C_{\mathrm{ins\_wt}} + N_{\mathrm{R\_Bat}} \times C_{\mathrm{rep\_Bat}} \tag{30}$$

$$C_{\mathrm{INV}} = C_{\mathrm{cap\_inv}} + C_{\mathrm{ins\_inv}} + T_{\mathrm{lifetime}} \times C_{\mathrm{O\&M\_inv}} + N_{\mathrm{R\_inv}} \times C_{\mathrm{rep\_inv}} \tag{31}$$

$$C_{\mathrm{CON}} = C_{\mathrm{cap\_con}} + C_{\mathrm{ins\_con}} + T_{\mathrm{lifetime}} \times C_{\mathrm{O\&M\_con}} + N_{\mathrm{R\_con}} \times C_{\mathrm{rep\_con}} \tag{32}$$

$$C_{\mathrm{DG}} = C_{\mathrm{cap\_DG}} + C_{\mathrm{f\_DG}} + T_{\mathrm{life}} \times C_{\mathrm{O\&M\_DG}} + C_{\mathrm{em}} + N_{\mathrm{R\_DG}} \times C_{\mathrm{rep\_DG}} \tag{33}$$

where N_R is the number of component replacements through the lifetime period. In this study, the lifetime of both wind turbine and PV modules is assumed to be 20 year, the lifetime for both controller and inverter is assumed as 10 years, and the lifetime for the batteries is assumed to be 5 years [28]. The replacement costs C_{rep} of the components are considered to be equal to their capital costs.

4.2. Design constraints

Due to physical and operational limits of the studied system, there is a set of constraints that should be satisfied for any feasible solution.

4.2.1. Constraint 1: power balance constraint

The total amount of electricity generation in terms of kWh/year must meet or exceed the total effective energy consumption of the load. The annual effective energy consumption can be derived as the annual energy consumption of the load divided by the system efficiency.

$$\sum_i E_{PV} N_{PV} + \sum_j E_{WT} N_{WT+} \sum_k E_{DG} N_{DG} \geq E_{eff} \quad (34)$$

$$E_{eff} = \frac{E_{load}}{\eta} \quad (35)$$

$$\eta = \eta_{INV} \times \eta_{CON} \times \eta_W \times \eta_{BAT} \times \eta_{DG} \quad (36)$$

where E_{eff}—effective energy consumption, (kWh/year); E_{load}—annual energy consumption, (kWh/year); E_{PV}—annual generated energy by PV modules, (kWh/year); E_{WT}—annual generated energy by wind turbines, (kWh/year); E_{DG}—annual generated energy by diesel generators, (kWh/year); η—system efficiency; η_{INV}—inverter efficiency; η_{CON}—controller efficiency; η_w—connection wires efficiency; η_{BAT}—battery efficiency; and η_{DG}—diesel generator efficiency.

In case of wind/PV/battery scenario, the number of diesel generator units in (34) is taken as zero and the diesel generator efficiency in (36) is taken as 1. For the wind/PV/diesel scenario, the battery efficiency in (36) is taken as 1. The average efficiency for inverter, controllers, wires, battery, and diesel generator are shown in Table 1.

4.2.2. Constraints 2: bounds of design variables

These constraints include physical constraints on the number of wind turbine unites, PV modules, and diesel units due to the available land area.

The area of land allocated in the project to install the concrete bases of wind turbines towers or solar cells holders is 50 m^2. This area is enough for 10 solar cells holders, taking into account the shadow calculations and five concrete bases for wind turbines and eight units of diesel generators. Therefore, five wind turbines, 10 PVs, and eight diesel generators have been taken as a maximum limit for this constraint.

It also includes constraints regards to the sizing of inverters and controllers and the state of charge of batteries.

Table 1
Average efficiency of hybrid system components

Component	Efficiency
Inverter	0.95
Controller	0.95
Wires	0.90
Battery	0.85
Diesel	0.85

$$0 < N_W \leq N_{W_{max}} \quad (37)$$

$$0 < N_{PV} \leq N_{PV_{max}} \quad (38)$$

$$0 \leq N_{DG} \leq N_{DG_{max}} \quad (39)$$

$$\sum_g P_{IN} N_{IN} \geq P_{max} \quad (40)$$

$$\sum_k P_{CON} N_{CON} \geq P_{PV_{max}} \quad (41)$$

$$SOC_{min} \leq SOC \leq SOC_{max} \quad (42)$$

where N_{Wmax}—maximum number of wind turbines; N_{PVmax}—maximum number of PV modules; N_{DGmax}—maximum number of diesel units; P_{IN}—maximum output power of inverter, (W); P_{CON}—maximum output power of controller, (W); P_{max}—maximum load, (W); P_{PVmax}—PV maximum power at STC, (W); SOC—Battery state of charge.

4.2.3. Constraint 3: limits of diesel operation

The diesel generator should have time limits of operation to reduce wear and tear [29].

$$\sum_{t=1}^{24} t \leq T_{DG} \quad (43)$$

$$0 \leq T_{DG} \leq K \quad (44)$$

where K is the maximum permissible time to operate the generator daily and T_{DG} represents the number of daily running hours.

The parameter used to measure the pollutant emission is the amount of CO_2. It represents the large percentage of the emission of fuel combustion.

Up till now there are no maximum allowable limits of CO_2 emissions in any production sector in Egypt. In this study, a maximum allowable limit of CO_2 in Egypt is assumed to investigate the impact of CO_2 on the optimal system configuration and TIC.

$$CO_2 \leq CO_{2max} \quad (45)$$

The formulated optimization problem is solved using MPSO technique to obtain the number of PV modules, wind turbines, batteries, inverters, controllers, and diesel units which minimize the annual TIC considering CO_2 emissions.

5. Hybrid system optimization model using proposed MPSO technique

In a previous work, the authors have proposed a general PSO modification for electrical applications [30]. The proposed modified PSO technique can determine the optimal PSO initial vectors and parameters to make PSO faster, performable, and more accurate. By implementing the proposed MPSO technique we get the optimum initial parameters that make the results converge faster. In this case the optimum initial parameters are: maximum number of particles = 45; weight factor = 0.95; and maximum iteration number = 75.

The computational procedure of the proposed MPSO method for optimal sizing of hybrid system is shown in Fig. 3 and can be explained as follows:

Step 1: Enter input data: the typical meteorological annual data, the technical and economical data for each component of the hybrid system, the annual electrical power demand by the load, and the MPSO parameters.

Step 2: Select the design scenario (PV/Wind/Battery or PV/Wind/Diesel or PV/Wind/Battery/Diesel).

Step 3: Calculate the annual produced energy for the hybrid system using (4), (12), (24), and the battery bank capacity using (13).

Step 4: Generate N particles; for each particle *i*, choose initial position vector, *Xi*(0), and velocity, *Vi*(0), (initial vector of HRES components number) randomly and set it as best position of particle *Pi*(0) of particle *i*.

Step 5: For each particle, calculate the random value of TIC using (21).

Step 6: If the particle *achieves all constraints* go to step 7. Otherwise, particle is infeasible. Go to step 5.

Step 7: Compare particle objective value with the individual P_{best}, if the objective value is lower than current P_{best}, set this value as the new P_{best}.

Step 8: Choose the particle associated with the minimum individual P_{best} of all particles, and set the value of this P_{best} as the current overall g_{best}.

Step 9: Update the velocity and position of particle.

Step 10: If any of the following stopping criteria (maximum number of iterations or maximum change in objective function value, or maximum computational time is reached), then go to Step 11. Otherwise, go to Step 5.

Step 11: Obtain the minimum value of TIC.

6. Numerical application

The main objective of this study was to design an optimum and efficient hybrid system to feed a small-scale brackish RO desalination unit and a tourism motel located in Hurghada, Egypt. The developed Matlab code is implemented for the three prescribed scenarios and the results are compared to each others to select the optimum combination of the hybrid system.

6.1. Input module

The input data, in this study, includes the load data, meteorological data for Hurghada city, and techno-economic data of hybrid system components.

6.1.1. Load data

The brackish water reverse osmosis load is assumed to operate for 12 h in summer and 10 h in winter. Also, the motel is populated by approximately 20 inhabitants (15 guests and five workers) and includes a kitchen, a small garden, and a small swimming pool. The amount of water consumed by 20 motel inhabitants and the amount of water required for the daily operation of the motel which is calculated to be around 5 m^3/d.

In this study the annual load is assumed to vary between summer and winter as explained by Table 2. Fig. 4 shows the estimated daily load variations for the studied system with a peak load of 5.32 kW and an average daily consumption of 46.56 kWh.

6.1.2. Meteorological data

Hurghada city is located at 27° 15′ 26′′ N latitude, 33° 48′ 46′′ E longitude, elevation 1 m and Red Sea climate district. The city is characterized by an intensive solar radiation. Wind is also an abundant resource. The monthly average wind speed and solar radiation are obtained from NASA surface meteorology and solar energy [31]. Table 3 shows the monthly average insulation incident on a horizontal surface. As explained in Section 3.1, it is necessary to adjust the wind speed to the hub height if the speed is measured at a height different than that of turbine hub height using (2). In this study, the wind towers are taken with a height of 20 m, so that the measured wind speed values have to be modified. Table 4 shows the monthly average wind speed at 50 m and the corresponding modified wind speed at 20 m height.

6.1.3. Techno-economical data of system components

The techno-economical data of the selected commercial components used in this study are shown in Appendix A [32–35].

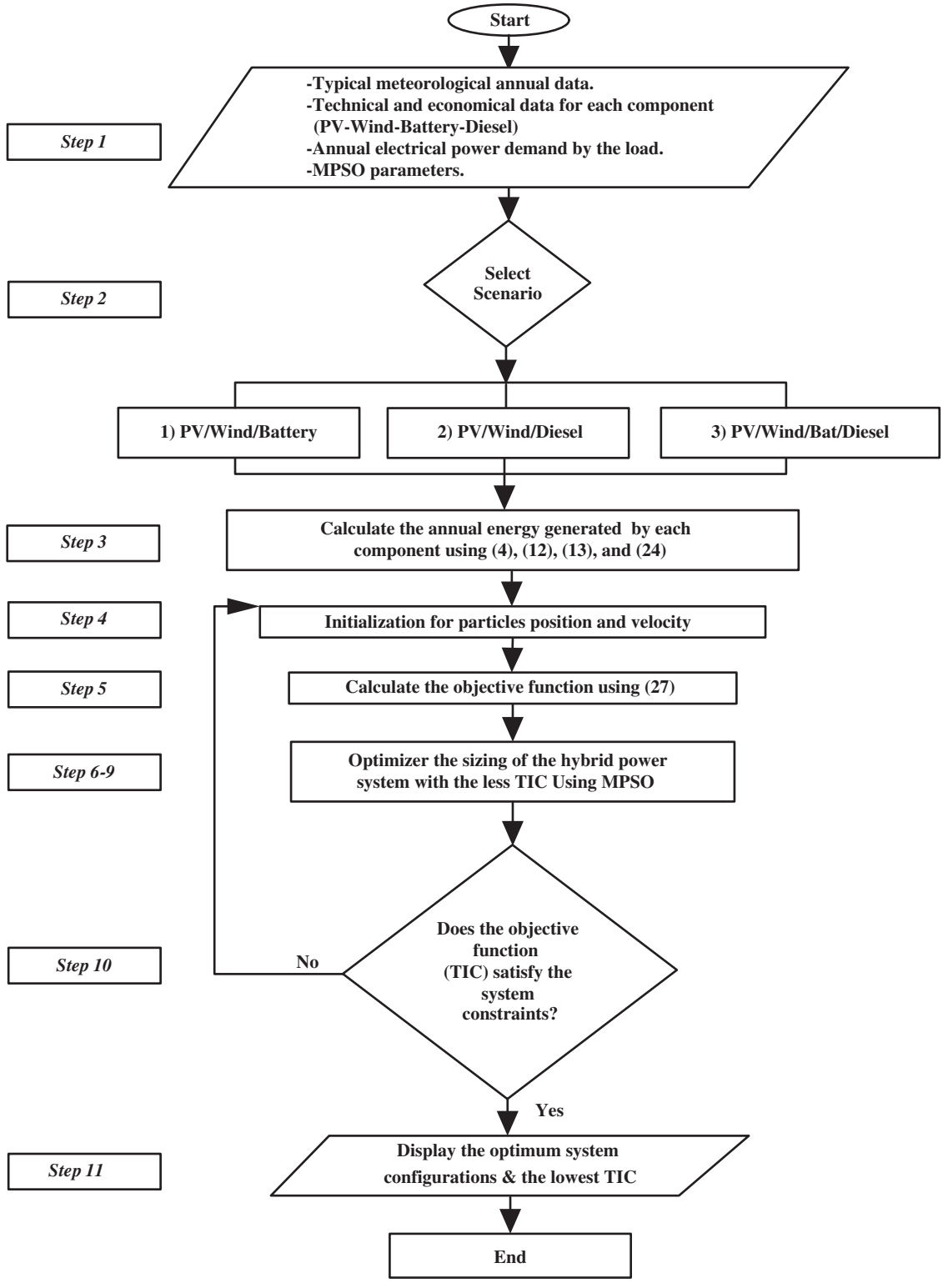

Fig. 3. Hybrid system optimization model using proposed MPSO technique flowchart.

Table 2
Daily electrical load requirements

Appliance	Number of units	Rated power (W)	Operation period for winter load (h)	Operation period for summer load (h)
Reverse osmosis unit	1	1,800	10	12
TV	1	80	10	12
Refrigerator	1	100	20	24
Lighting	22	20	12	12
Fans	18	100	–	14
Washing machine	1	1,000	4	6
Blower	1	100	6	10

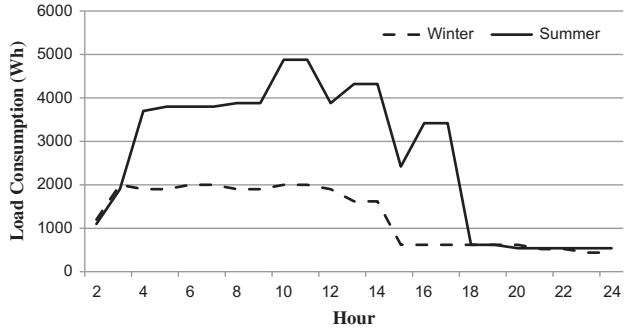

Fig. 4. Daily load variations for the studied system.

6.2. Optimization module

The proposed method is applied to optimally design the required hybrid energy system. The input data to the Matlab code are the load data, the meteorological data of the studied site, the techno-economical data of the system components, the predefined constraints, MPSO fitness function, and MPSO specific parameters. These parameters are the following: maximum iteration number = 75, number of particles = 45, and weight factor = 0.95.

6.3. Optimization results

The optimization problem is performed to obtain the optimum power system configuration that meets the previously mentioned load profile for the three prescribed scenarios. The results are compared to determine the best combination with minimum investment cost. The simulation results of the three scenarios are displayed in Tables 5a–5c. The TIC for the three proposed scenarios are \$21686.6924 for wind/PV/battery scenario, \$16372.1414 for wind/PV/diesel scenario, and \$20951.5064 for wind/PV/battery/diesel scenario.

6.3.1. Result analysis

In the first scenario, there are two generation sources (wind/PV); the two sources share the load. The optimal solution is obtained with five wind turbines and five PV units with different capacities. In this case the total annual generated energy is 24292.778 kWh, whereas the annual consumed energy is 24277.66 kWh. The surplus energy is lost in batteries charging/discharging processes.

In the second scenario, there are three generation sources (wind/PV/diesel). The number of wind turbines decreases to three units. This decrease is a result of the presence of the diesel generators as they share the load and run 6 h daily. In this case the total annual generating energy is 24297.278 kWh, whereas the annual consumed energy is 24277.66 kWh. This scenario represents the most economic hybrid system configuration with a TIC of \$16372.1414.

In the third scenario, the value of annual effective consumed energy increases to 28561.953 kWh due to the decrease in system efficiency. Therefore, the amount of generated energy increases to 28839.75 kWh. The number of PVs decreases to one unit due to the presence of diesel generators.

Fig. 5 shows the share of PV, wind, and diesel in producing the demand electricity for scenario 2 (optimal scenario). Without any constraints on the CO_2 emission, the diesel generators carry out the largest part of the load. In the next item we will investigate the impact of CO_2 emission on the optimal system configuration and the TIC.

Table 3
Monthly averaged insulation incident on a horizontal surface for Hurghada city

Month	January	February	March	April	May	June	July	August	September	October	November	December
Solar radiation[a] ($kWh/m^2/d$)	4.2	5.7	6.3	7.5	8	8.3	8.2	7.8	7	5.8	4.4	4

[a]22-year average solar radiation.

Table 4
Monthly averaged wind speed for Hurghada city

Month	January	February	March	April	May	June	July	August	September	October	November	December
Wind speed[a] (m/s) (measured at 50 m height)	7.2	7.1	7	6.3	7.3	7.8	6.8	7.2	7.3	5.7	6.7	6.8
Modified wind speed (at 20 m height)	6.32	6.23	6.14	5.53	6.40	6.84	5.97	6.32	6.40	5.00	5.88	5.97

[a]10-year average wind speed.

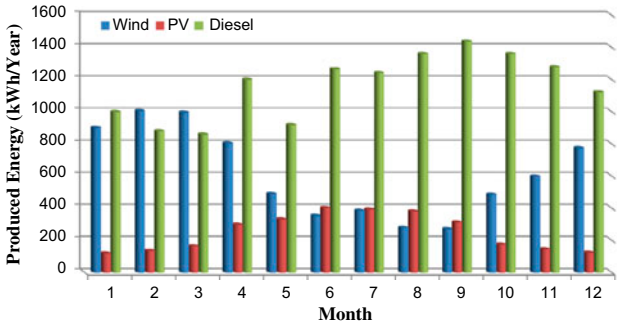

Fig. 5. Load sharing for scenario 2.

6.3.2. Impact of CO_2 emission on TIC

In this section, impacts of different CO_2's constraint on the TIC and hybrid system components are examined. As explained before there are no maximum allowable limits of CO_2 emissions in Egypt. To study the impact of CO_2 emission on TIC, three different maximum allowable CO_2 values are assumed as explained in Table 6. It can be observed that decreasing the maximum allowable CO_2 limits results in decreasing the number of diesel generators and consequently increasing the number of wind turbines. Increasing the number of wind turbines will increase

Table 5a
Optimization sizing results for scenario 1 (wind/PV/battery)

Hybrid system component	Commercial type	Total number	Rated capacity (W)	Total capacity (W)	Total annual energy generated (kWh/year)
Wind turbines	Southwest (Whisper 200)	1	1,000	1,000	4932.5
	Southwest (Skystream 3.7)	1	1,800	1,800	9016.6
	Aeromax Engineering (Lakota)	1	800	800	3162.05
	Bornay (Inclin 250)	1	250	250	1412.6
	Bornay (Inclin 600)	1	600	600	2777.4
Photovoltaics	Lightway 235 W	3	235	705	1671.89
	CSI CS6X-280P	2	280	560	1319.738
Battery	US Battery US250	4	250 Ah	–	–
Inverter	Schneider Electric (DR1524E)	4	1,500	6,000	–
Controller	Schneider Electric (XW-MPPT-60)	1	1,500	1,500	–
TIC = $21686.6924					

Table 5b
Optimization sizing results for scenario 2 (wind/PV/diesel)

HYBRID system component	Commercial type	Total number	Rated capacity (W)	Total capacity (W)	Total annual energy generated (kWh/year)
Wind turbines	Aeromax Engineering (Lakota)	1	800	800	3162.05
	Bornay (Inclin 250)	1	250	250	1412.6
	Bornay (Inclin 600)	1	600	600	2777.4
Photovoltaics	Lightway 235 W	3	235	705	1671.89
	CSI CS6X-280P	2	280	560	1319.738
Diesel generator	STEPHIL (SE 3000D)	4	1,900	7,600	13953.6
Inverter	Schneider Electric (DR1524E)	4	1,500	6,000	–
Controller	Schneider Electric (XW-MPPT-60)	1	1,500	1,500	–
TIC = $16372.1414					

Table 5c
Optimization sizing results for scenario 3 (wind/PV/battery/diesel)

HYBRID system component	Commercial type	Total number	Rated capacity (W)	Total capacity (W)	Total annual energy generated (kWh/year)
Wind turbines	Aeromax Engineering (Lakota)	1	800	800	3162.05
	Bornay (Inclin 250)	1	250	250	1412.6
	Bornay (Inclin 600)	1	600	600	2777.4
Photovoltaics	Lightway 235 W	1	235	235	557.3
Diesel generator	STEPHIL (SE 3000D)	6	1,900	11,400	20930.4
Battery	US Battery US250	2	250 Ah	–	–
Inverter	Schneider Electric (DR1524E)	4	1,500	6,000	–
Controller	Schneider Electric (XW-MPPT-60)	1	1,500	1,500	–
TIC = $20951.5064					

Table 6
Comparison between different CO_2 constraints for scenario 2

		Maximum CO_2 emission		
Item	No. of CO_2 limits	8,000 kg	5,000 kg	3,000 kg
No. of wind turbines	3	3	5	4
No. of PV modules	5	12	7	8
No. of diesel generators	4	3	2	1
No. of controllers	1	2	1	1
No. of inverters	4	4	4	4
Wind energy (kWh/year)	7352.05	7352.05	13300.17	16368.65
PV energy (kWh/year)	2991.628	6687.56	5631.112	4458.373
Diesel gen. energy (kWh/year)	13953.6	10465.2	6976.8	3488.4
TIC ($/year)	16372.1414	16842.9245	17188.5688	17296.5343
Annual cost of energy ($/kWh)	0.673826155	0.687331365	0.66344428	0.711340054
CO_2 emissions (kg/year)	9837.288	7377.966	4918.644	2459.322

the installation cost of the system and accordingly increase the system TIC.

7. Conclusion

This study proposed an MPSO-based technique for modeling and optimization of a hybrid system to supply a load of small-scale brackish reverse osmosis desalination unit. A Matlab code was developed for solving the optimization problem to minimize the annual TIC considering CO_2 emissions cost.

Three proposed scenarios were investigated and compared to detect the most economical hybrid system configuration. These scenarios include wind/PV/battery, wind/PV/diesel, and wind/PV/ battery/diesel configurations. The wind/PV/diesel system, offers the most economic scenario with the lowest TIC. To reduce the greenhouse effect, an economic study for the effect of maximum allowable CO_2 emissions was implemented. Different maximum allowable CO_2 values were assumed to study the impact of CO_2 emission on TIC, as there are no maximum allowable limits of CO_2 emissions in Egypt up till now. The study shows that decreasing the maximum allowable CO_2 limits results in decreasing the number of diesel generators and increasing the system TIC.

References

[1] Future Directions International (NREA), The Future of Food and Water Security in New Egypt, 2012. Available from: <http://www.futuredirections.org.au/publications/food-and-water-crises/813-the-future-of-food-and-water-security-in-new-egypt.html>, Last accessed April 2015.
[2] A. Al-Karaghouli, D. Renne, L. Kazmerski, Solar and wind opportunities for water desalination in the Arab

regions, Renewable Sustainable Energy Rev. 13 (2009) 2397–2407.
[3] P. Bajpai, V. Dash, Hybrid renewable energy systems for power generation in stand-alone applications: A review, Renewable Sustainable Energy Rev. 16 (2012) 2926–2939.
[4] A. Kershman, J. Rheinlander, T. Neumann, O. Goebel, Hybrid wind/PV and conventional power for desalination in Libya—GECOL's facility for medium and small scale research at Ras Ejder, Desalination 183 (2005) 1–12.
[5] I. Spyrou, J. Anagnostopoulos, Design study of a stand-alone desalination system powered by renewable energy sources and a pumped storage unit, Desalination 257 (2010) 137–149.
[6] I. Yilmaz, M. Soylemez, Design and computer simulation on multi-effect evaporation seawater desalination system using hybrid renewable energy sources in Turkey, Desalination 291 (2012) 23–40.
[7] T. Barek, K. Bourouni, K. Ben Mohamed, Optimization coupling RO desalination unit to renewable energy by genetic algorithms, Desalin. Water Treat. 51 (2013) 1416–1428.
[8] G. Klise, J. Stein, Models Used to Assess the Performance of Photovoltaic Systems, Sandia National Laboratories, CA, 2009.
[9] L. Arribas, G. Bopp, M. Vetter, A. Lippkau, K. Mauch, World-wide overview of design and simulation tools for hybrid PV Systems, International Energy Agency, Photovoltaic Power Systems Program, Report IEA–PVPS T11-01 (2011).
[10] A. Khalifa, Evaluation of different hybrid power scenarios to reverse osmosis (RO) desalination units in isolated areas in Iraq, Energy Sustainable Dev. 15 (2011) 49–54.
[11] F. Fahmy, N. Ahmed, H. Farghally, Optimization of renewable energy power system for small scale brackish reverse osmosis desalination unit and a tourism motel in Egypt, Smart Grid Renewable Energy 3 (2012) 43–50.
[12] E. Mokheimer, A. Sahin, A. Al-Sharafi, A. Ali, Modeling and optimization of hybrid wind–solar-powered reverse osmosis water desalination system in Saudi Arabia, Energy Convers. Manage. 75 (2013) 86–97.
[13] R. Nagaraj, Renewable energy based small hybrid power system for desalination applications in remote locations, Power Electronics (IICPE), Kalpakkam, 2012, pp. 1–5.
[14] A. Mohamed, Design and cost analysis of hybrid renewable energy for water desalination in remote areas, Int. J. Sci. Res. (IJSR) 2 (2013) 342–345.
[15] A. Al-Karaghouli, L. Kazmerski, Economic analysis of a brackish water photovoltaic-operated (BWRO-PV) desalination system, World Renewable Energy Congress XI, Abu Dhabi, 2010.
[16] D. Kumar, B. Dash, A. Akella, Optimization of PV/wind/micro-hydro/diesel hybrid power system in HOMER for the study area, Int. J. Electr. Eng. Inf. 3 (2011) 307–325.
[17] A. Hassan, M. EL-Saadawi, M. Kandil, M. Saeed, A particle swarm optimization based approach for optimal sizing of stand-alone hybrid renewable energy systems, The 16th International Middle-East Power System Conference (MEPCON'14), Cairo, 2014.
[18] M. Danish, F. Al Asfour, N. Al-Najem, Energy consumption in equivalent work by different desalting methods: Case study for Kuwait, Desalination 151 (2003) 83–92.
[19] M. Rivera, Small Wind/Photovoltaic Hybrid Renewable Energy System Optimization, M.Sc., University of Puerto Rico, 2008.
[20] E. Koutroulis, D. Kolokotsa, A. Potirakis, K. Kalaitzakis, Methodology for optimal sizing of stand-alone photovoltaic/wind-generator systems using genetic algorithms, Solar Energy 80 (2006) 1072–1088.
[21] M. Yazdanpanah, Modeling and sizing optimization of hybrid photovoltaic/wind power generation system, J. Ind. Eng. Int. 10 (2014) 1–14.
[22] Solar Energy International, Photovoltaic Design and Installation Manual, New Society, Carbondale, 2007.
[23] A. Hassan, M. Saadawi, M. Kandil, M. Saeed, Modified particle swarm optimisation technique for optimal design of small renewable energy system supplying a specific load at Mansoura University, IET Renewable Power Gener. 9 (2015) 1–10.
[24] B. Bilal, V. Sambou, C. Kébé, P. Ndiaye, M. Ndongo, Methodology to size an optimal stand-alone PV/wind/diesel/battery system minimizing the levelized cost of energy and the CO_2 emissions, Energy Procedia 14 (2012) 1636–1647.
[25] Central Agency for Public Mobilization and Statistics, Egypt in Figures, Report, 14, 2014. Available from: <http://www.capmas.gov.eg/pdf/EgyptinFigures2014/pages/english%20Link.htm>, Last accessed April 2015.
[26] Intergovernmental Panel on Climate Change IPCC, Safeguarding the Ozone Layer and the Global Climate System: Issues Related to Hydro Fluorocarbons and Per Fluorocarbons, A Special Report, 2005.
[27] S. El-Mowafy, Environmental and Health Impacts Resulting from Fossil Fuels as an Energy Source in Egypt, A Report Submitted to Egyptian Environmental Affairs Agency (in Arabic) (2014). Available from: <http://www.eeaa.gov.eg/arabic/main/env_ind_energy.asp>, Last accessed April 2015.
[28] A. Anayochukwu, Feasibility assessment of a PV-diesel hybrid power system for an isolated of-grid Catholic Church, Electron. J. Energy Environ. 1 (2013) 49–63.
[29] A. Gupta, R. Saini, M. Sharma, Modelling of hybrid system Part I: Problem formulation and model development, Renewable Energy 36 (2011) 459–465.
[30] M. El-Saadawi, A. Hassan, M. Saeed, A general PSO modification for electrical applications, J. Electr. Control Eng. 1 (2011) 25–28.
[31] NASA Surface meteorology and Solar Energy. Available from: <https://eosweb.larc.nasa.gov/sse/>, Last accessed April 2015.
[32] Alternative Energy Store. Available from: <http://www.altestore.com/store/>, Last accessed April 2015.
[33] Affordable-solar Whole Sale Distribution. Available from: <http://www.affordable-solar.com/>, Last accessed April 2015.
[34] CIVICSOLAR. Available from: <http://www.civicsolar.com/>, Last accessed April 2015.
[35] Just Generators. Available from: <http://www.justgenerators.co.uk/pages/dieselrange.htm>, Last accessed April 2015.

Appendix A. Hybrid system components techno-economic data [32–35]

A.1. Wind turbines [32]

Product	Rated output (W)	C_{cap} ($)	C_{ins} ($)	$C_{O\&M}$ ($/year)
Southwest (Air X)	400	248.985	74.6955	24.8985
Southwest (Whisper 100)	900	844.985	253.4955	84.4985
Southwest (Whisper 200)	1,000	1000	300	100
Southwest (Whisper 500)	3,000	3076.391	922.9173	307.6391
Southwest (Skystream 3.7)	1,800	1824.47	547.341	182.447
Aeromax Engineering (Lakota)	800	412.82	123.846	41.282
Bergey (BWC 1500)	1,500	1706.315	511.8945	170.6315
Bergey (BWC XL.1)	1,000	1494.57	448.371	149.457
Bergey (BWC Excel-R)	8,100	11198.43	3359.529	1119.843
Bornay (Inclin 250)	250	165.4001	49.62003	16.54001
Bornay (Inclin 600)	600	394.3901	118.317	39.43901
Bornay (Inclin 1500)	1,500	2792.885	837.8655	279.2885
Bornay (Inclin 3000)	3,000	4191.035	1257.311	419.1035
Bornay (Inclin 6000)	6,000	6783.701	2035.11	678.3701
Abundant Renewable (ARE110)	2,500	2740.001	822.0003	274.0001
Abundant Renewable (ARE442)	10,000	13199	3959.7	1319.9
Kestrel Wind (600)	600	844.92	253.476	84.492
Kestrel Wind (800)	800	986.24	295.872	98.624
Kestrel Wind (1000)	1,000	1545.135	463.5405	154.5135
Kestrel Wind (3000)	3,000	3001.125	900.3375	300.1125
Solacity (Eoltec)	6,000	7497.5	2249.25	749.75

A.2. Controllers [33,34]

Manufacture	Model	P_{out} (W)	C_{cap} ($)	C_{ins} ($)	$C_{O\&M}$ ($/year)	C_{rep} ($)
Schneider Electric	XW-MPPT-60	1,500	248	4.96	0.745335	248
Outback	FM 80	2,000	335	6.7	1.005	335
Outback	FM 60	1,500	280	5.6	0.84	280
Schneider Electric	XW-MPPT-80	2,000	580	11.6	1.739835	580
Blue Sky	SB3048	750	173	3.46	0.519	173

A.3. Inverters [33,34]

Manufacture	Model	P_{out} (W)	C_{cap} ($)	C_{ins} ($)	$C_{O\&M}$ ($/year)	C_{rep} ($)
Schneider Electric	DR1524E	1,500	350	7.15	1.95	350
Schneider Electric	XW6048	6,000	1518	30.375	4.6	1518
Schneider Electric	XW4548	4,500	1216.43	24.3286	3.64929	1216.43
Outback	FX2024ET	2,000	654.5	13.09	1.9635	654.5
Schneider Electric	XW4024	4,000	812.05	24.2386	2.43615	812.05

A.4. PV panels [33,34]

Product	η	P_{out} at 1000 W/m^2	C_{cap} ($)	C_{ins} ($)	$C_{O\&M}$ ($/year)
Sharp ND-250QCS	0.153	250	240	108	6
Hyundai HiS-255MG	0.160	255	229.5	103.275	5.7375
Lightway	0.140	235	157.45	70.8525	3.93625
Trina TSM-PA05	0.150	240	165.6	74.52	4.14
Solartech SPM135P	0.135	135	359.1	161.595	8.9775
CSI CS6P-235PX	0.146	235	169.2	76.14	4.23
CSI CS6X-280P	0.146	280	207.2	93.24	5.18
CSI CS6X-285P	0.150	285	219.23	98.6535	5.48075
Canadian Solar CS6P	0.160	250	198.75	89.4375	4.96875
CSI CS6X-295P	0.154	295	244.85	110.1825	6.12125
Canadian Solar CS6X-300P	0.156	300	249	112.05	6.225
Canadian Solar CS6P-255M	0.158	255	230.77	103.8465	5.76925
Hyundai HiS-260MG	0.161	260	238.08	107.136	5.952

A.5. Batteries [34]

Product	Ah	C_{cap} ($)	C_{ins} ($)	C_{rep} ($)
MK 8L16	370	1749.3	35.7	1749.3
Surrette 12-Cs-11Ps	357	6851.425	139.825	6851.425
Surrette 2Ks33Ps	1,765	5434.492	110.908	5434.492
Surrette 4-CS-17PS	546	3935.925	80.325	3935.925
Surrette 4-Ks-21Ps	1,104	6804.777	138.873	6804.777
Surrette 4-Ks-25Ps	1,350	8524.922	173.978	8524.922
Surrette 6-Cs-17Ps	546	5551.112	113.288	5551.112
Surrette 6-Cs-21Ps	683	6501.565	132.685	6501.565
Surrette 6-Cs-25Ps	820	7784.385	158.865	7784.385
Surrette 8-Cs-17Ps	546	7492.835	152.915	7492.835
Surrette 8-Cs-25Ps	820	10350.03	211.225	10350.03
Surrette S-460	350	1976.709	40.341	1976.709
Surrette S-530	400	2186.625	44.625	2186.625
Trojan L16H	420	2099.16	42.84	2099.16
Trojan T-105	225	991.27	20.23	991.27
US Battery US185	195	1667.666	34.034	1667.666
US Battery Us2200	225	1032.087	21.063	1032.087
US Battery US250	250	979.608	19.992	979.608
Surrette S-460	350	1749.3	35.7	1749.3
Surrette S-530 6V	400	1900.906	38.794	1900.906

A.6. Diesel generators [35]

Manufacture	Model	P_{out} (kW)	C_{cap} ($)	$C_{O\&M}$ ($/h)	Fuel consumption (L/h)	Lifetime (h)
STEPHIL	SE 3000D	1.9	1713.15	0.2	0.7	8,760